Stress Corrosion Cracking of X70 Pipeline Steel immersed in Synthetic Soil solution

R. Galván-Martínez[1], A. Carmona[2], M. Baltazar[2], A. Contreras[3] y R. Orozco-Cruz[1]*
[1] Unidad Anticorrosión, Instituto de Ingeniería, Universidad Veracruzana, Veracruz, México.
[2] Facultad de Ingeniería Civil - Xalapa, Universidad Veracruzana, Veracruz, México.
[3] Instituto Mexicano del Petróleo, Eje Central Lázaro Cárdenas Norte No.152, Cd. México, México.

Agrietamiento por corrosión y esfuerzo de un acero de tubería X70 inmerso en una solución sintética de suelo

Esquerdament per corrosió i esforç d'un acer X70 submergits en una solució sintètica d'aigua del terra

RECEIVED: 22 MAY 2018; REVISED: 5 JULY 2018; ACCEPTED: 18 JULY 2018

SUMMARY

A study of stress corrosion cracking (SCC) susceptibility of API X70 pipeline steel exposed to a synthetic soil solution at room temperature and atmospheric pressure through slow strain rate tests (SSRT) was carried out. Electrochemical noise (EN) measurements were recorded during SSRT in order to study the SCC process. Additionally, polarization curves (PC) to evaluate the corrosion were carried out. Characteristic current transients were identified and assigned to different processes. EN measurements were analyzed in the time and frequency domain. The currents transients and localization index (LI) indicate that at the beginning of the test, in the elastic and yielding strength zone, the corrosion is dominant by not much transients with low amplitude and frequency. At the maximum strength (UTS) and before fracture, the presence of transients increased. The highest corrosion rate, obtained by R_n and Z_n, were obtained in the plastic zone before of the facture. A superficial analysis obtained by scanning electron microscopy (SEM) was carried out on surface of the samples and it revealed the presence of some micro-cracking in the gage section of SSRT specimens. According to SCC index and SEM observations the X70 steel has low SCC susceptibility at the conditions studied.

Keywords*:* Stress corrosion cracking (SCC); electrochemical noise (EN); polarization curves (PC); slow strain rate tests (SSRT), X70 steel.

RESUMEN

Se ha llevado a cabo un estudio de la susceptibilidad al agrietamiento por corrosión y esfuerzo (SCC) del acero de tubería API X70 expuesto a una solución sintética de agua del suelo a temperatura ambiente y a presión atmosférica y se han utilizado pruebas a baja velocidad de deformación (SSRT). Las mediciones de ruido electroquímico (EN) se registraban durante las SSRT con el objetivo de estudiar el proceso de SCC. Adicionalmente, se llevaban a cabo las curvas de polarización (PC) para evaluar la corrosión. Se identificaban corrientes transitorias y se asignaban a diferentes procesos. Las mediciones EN se analizaban en el dominio de tiempo y frecuencia. Los transientes de corriente e índice de localización indicaron que al inicio de la prueba en la zona elástica y en la zona de cedencia, la corrosión es dominada por algunos transientes de baja amplitud y frecuencia. En el punto de resistencia máximo (UTS) y antes de la fractura, aumentaba la presencia de fenómenos transitorios. Las velocidades de corrosión más elevadas, obtenidas por Rn y Zn, se alcanzaban en la zona plástica antes de la fractura. Un análisis superficial obtenido mediante microscopía electrónica de barrido (SEM) se llevaba a cabo en la superficie de las muestras y revelaba la presencia de algunas microgrietas en la sección calibrada de las muestras SSRT. De acuerdo con el índice SCC y las observaciones SEM el acero X70 tiene baja susceptibilidad SCC en las condiciones estudiadas.

Palabras clave: Agrietamiento por corrosión y esfuerzo (SCC); ruido electroquímico (EN); curvas de polarización (PC); pruebas de tensión a baja velocidad de deformación (SSRT); acero X70.

***Corresponding author: rigalvan@uv.mx**

RESUM

S'ha dut a terme un estudi de la susceptibilitat per corrosió de fissuració deguda a tensions (SCC) del acer de tubs API X70 exposat a una solució sintètica d'aigua del terra a temperatura ambient i a pressió atmosfèrica i s'han utilitzat probes o tests a una velocitat baixa de deformació (SSRT). Les medicions del soroll electroquímic (EN) es registraven durant les SSRT amb l'objectiu d'estudiar el procés SCC. Addicionalment, es portaven a terme les corbes de polarització (PC) per avaluar la corrosió. S'identificaven corrents transitòries i s'assignaven a diferents processos. Les medicions EN eren analitzades en el domini de temps i freqüència. Les corrents transitòries i l'índex de localització (LI) indican que al inici de la prova, en la zona del límit elàstic o resistència a la elongació, la corrosió està dominada per fenòmens transitoris de baixa amplitud i freqüència. En el punt de resistència màxim (UTS) i abans de la fractura, s'incrementava la presencia de fenòmens transitoris. Les velocitats de corrosió mes elevades, obtingudes per Rn i Zn, es trobaven a la zona plàstica abans de la fractura. Una anàlisi superficial obtinguda mitjançant microscòpia electrònica de rastreig (SEM) es portava a terme en la superfície de les mostres i revelava la presencia de micro-cracking en la secció de calibrat de les mostres SSRT. D'acord amb l'índex SCC i les observacions SEM l'acer X70 te baixa susceptibilitat SCC en les condicions estudiades.

Paraules clau: Corrosió de fissuració deguda a tensions (SCC); soroll electroquímic (EN); corbes de polarització (PC); proves a baixa velocitat de deformació (SSRT); acer X70.

1. INTRODUCTION

The stress corrosion cracking (SCC) is one of the most common cause of failure for buried pipelines steel transporting oil and its derivatives; one of the main factors of this fact, is the stress produced by operation pressure and the movement of the pipeline induced by the soil and its natural movement. [1,2] In addition, as the exposure time increase, the coating may deteriorate and detach, allowing that a corrosive medium may be in contact with the external surface of the pipeline. [3]

The conditions mentioned above induced two type of SCC in pipeline steel: 1) SCC at high pH, that it can occur by the generation of a concentrate solution of bicarbonates-carbonates (pH > 9) producing a localized corrosion with an intergranular crack morphology. The mechanism of this SCC is attributed to the selective anodic dissolution of the grain boundaries and to the rupture of the passive layer in the tip of the crack. On the other hand, the second type correspond to the SCC that it happen at almost neutral pH (6 to 8.5). This SCC has been associated to the diluted solutions generated by the underground water producing a localized corrosion with transgranular crack morphology. In this case, the mechanism is not well defined, but some studies indicate that the cracking may be attributed to the synergic effect between the anodic dissolution and the hydrogen embrittlement. [4-6]

Different electrochemical techniques have been used to estimate the risk of the SCC. The potentiodynamic polarization curves (PC) is one of these techniques; it has been used to predict the SCC process and to establish a susceptibility potential range in pipeline steel.[7] Another technique is the electrochemical noise (EN). This technique study the fluctuations of the potential and current generated by the corrosion process when the metal does not have any perturbation (at open circuit potential-OCP). [8]

The EN application to detect and monitoring the SCC process in laboratories is widely accepted by many researchers. Cottis *et a*l. [9] was one of the first researchers that reported the study of the SCC by EN. They measured and analyzed the noise of the current and potential generated by three different electrolyte-metal systems; they found an increment in the noise level generated by the sample under stress at the beginning of the cracks and a decrement of this noise level, as the crack propagates. In addition, Gonzales *et al.* [10] carried out some studies about the differences between general and localized corrosion in a steel immersed in thiosulfate solution. The analysis of the EN in the time domain showed current transients with high intensity and low frequency during the SCC process, this behavior indicated the presence of a localized corrosion type. On the other hand, when the steel was passivated and/or under uniform corrosion, current transients with low intensity and high frequency were found. It is important to point out that many studies of SCC using the EN technique has used the slow strain rate test machine mainly in stainless steel samples. [11-15] González [10,12] used the EN in order to detect the beginning and propagation of the cracks in SCC process in a martensitic stainless steel sample immersed in an acid and deaerated NaCl brine and correlated the potential transients with the nucleation and propagation of the cracks. Another technique used is the electrochemical emission spectroscopy (EES). This technique has been used in the study of corrosion processes. [14-16] The EES technique use the typical three electrodes array used in the EN study, but in this case, the second working electrode is a platinum (Pt) microelectrode. The EES is based in the supposition that the majority of the electrochemical noise is generated by the working electrode (for example stainless steel or carbon steel samples) and the noise generated by Pt is insignificant. This fact permit the study of the more active electrode. [17]

Contreras *et al.* [18] used this EES arrangement, with an X52 low carbon steel as working electro-

de in order to determine its susceptibility against SCC. In real time, he used the electrochemical noise for the corrosion analysis of this steel.

The focus of this investigation was to apply the electrochemical noise (EN) as a tool to detect stress corrosion cracking (SCC) in X70 pipeline steel exposed to a synthetic soil solution called NS4 at room temperature. The electrochemical potential and current noise were measured simultaneously during SSRT. Relation between EN and SCC process was analyzed.

2. EXPERIMENTAL PROCEDURE

2.1. Working electrode

The material used in the present study as working electrode was an API 5L X70 pipeline steel. Steel samples were obtained from a pipeline, which had an external diameter of 36 in. (914.4 mm) and wall thickness of 0.902 in. (22.91 mm). The samples used in the slow strain rate test were machined according to NACE TM 0198. [19] For EN measurements, cylindrical tensile samples obtained from X70 steel were used as working electrode.

2.2. Synthetic soil solution

A simulated ground water solution (called NS4) with pH 8 as the corrosive environment was used. NS4 synthetic solution has been widely used to simulate the soil solution in the study of near neutral pH-SCC behavior. Another synthetic soil solution like NS1, NS2, NS3, NS4, NOVA and C1 has been used in SCC studies. [20-22]

2.3. Experimental set up

The electrochemical measurements were carried out in a Potentiostat/Galvanostat using a typical electrochemical cell with a three electrodes array. The electrochemical techniques used were potentiodynamic polarization curves (PC) and electrochemical noise (EN). For EN measurements, SSRT specimens of X70 steel were used as working electrodes; the second working electrode was a platinum (Pt) microelectrode, while a saturated calomel electrode (SCE) was used as reference electrode. On the other hand, for PC the same electrochemical cell was used, but in this case, the platinum microelectrode was substituted by a sintered graphite rod and it was used as counter electrode.

2.4. Electrochemical measurements

In order to stabilize the redox reactions, the corrosion potential (E_{corr}) was measured during 20 minutes. It is important to point out that with this time, the Ecorr got a stable value indicating that the anodic and cathodic reaction have the same values. The electrochemical techniques used were potentiodynamic polarization curves (PC) and electrochemical noise (EN).

Polarization curves (PC)

They were recorded from -1.4 to 0 V vs SCE and the sweep rate from 50 and 0.5 $mV^{*}s^{-1}$. All PC were carried out at room temperature atmospheric pressure and without stress conditions.

Electrochemical noise (EN)

The sampling frequency was 1 Hz. Each measurement of EN consisted of 1200 data points and this was carried out at different exposure time. The EN data were analyzed in time and frequency domain. In time domain, the EN data were analyzed with the localized index (LI), noise resistance (Rn) and transients of current and potential. Meanwhile in frequency domain, the EN data were analyzed with the fast Fourier transform (FFT) and the maximum entropy method in order to get the noise impedance.

2.5. Slow Strain Rate Tests (SSRT)

SSRT were carried out on smooth cylindrical tensile samples, using a MCERT machine (Mobile Constant Extension Rate Tests) at strain rate of $1x10^{-6}$ s^{-1} in air and in a synthetic soil solution (NS4 solution). All SSRT were made at room temperature and atmospheric pressure. The length direction of the sample was parallel to the circumferential direction of the pipeline steel with the goal if cracks appear growth in the longitudinal direction of the pipe as is typically observed in underground pipelines. Cylindrical samples with a reduced length of 2.54 cm and 0.381 cm in diameter were machined with a total exposed area of 3.04 cm^2. After the SSRT was completed, the fractured sample was removed and prepared to SEM examination according to ASTM G1- 03. [23]

3. RESULTS AND DISCUSSION

3.1. Steel characterization

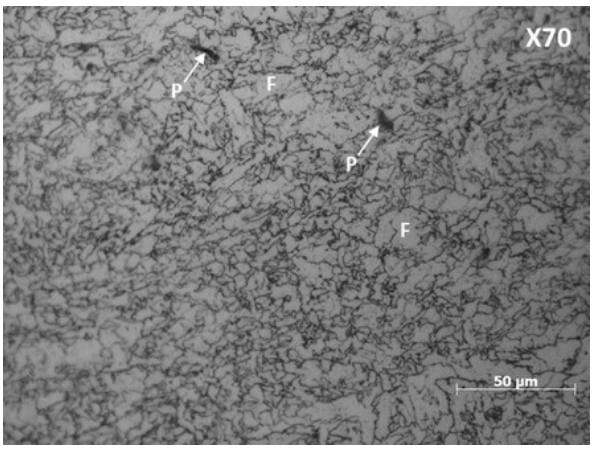

Figure 1. *Optical image of the microstructure of API X70 steel.*

In order to characterize the X70 pipeline steel, a microstructural analysis was carried out by optical microscopy (OM). Figure 1 shows that the microstructure is characterized by a mixture of fine and

coarse polygonal ferrite grains (F) with few dark perlite grains (P), typical of high strength low alloy steels. This steel has a grain size around 20 μm, containing little pearlite. Metallurgical factors (heat treatment, residual stress, inclusions and dislocations) and microstructures obtained (phases, microvoids, grains form and size) affect SCC. Many researchers have reported that uniform microstructures are beneficial to avoid SCC. [24-27] Low carbon steels produced through a thermo-mechanical controlled process are less susceptible to SCC. [25] SCC susceptibility depended basically of microstructures of the steel and not so much on the steel grade. Uniform microstructures, such as bainite or bainite-ferrite, were resistant to SCC, while inhomogeneous microstructures, such as ferrite-pearlite, were susceptible to SCC. This fact demonstrates that not only the steel grade must be considered in the SCC susceptibility, but rather the microstructure.

3.2. Slow Strain Rate Test (SSRT)

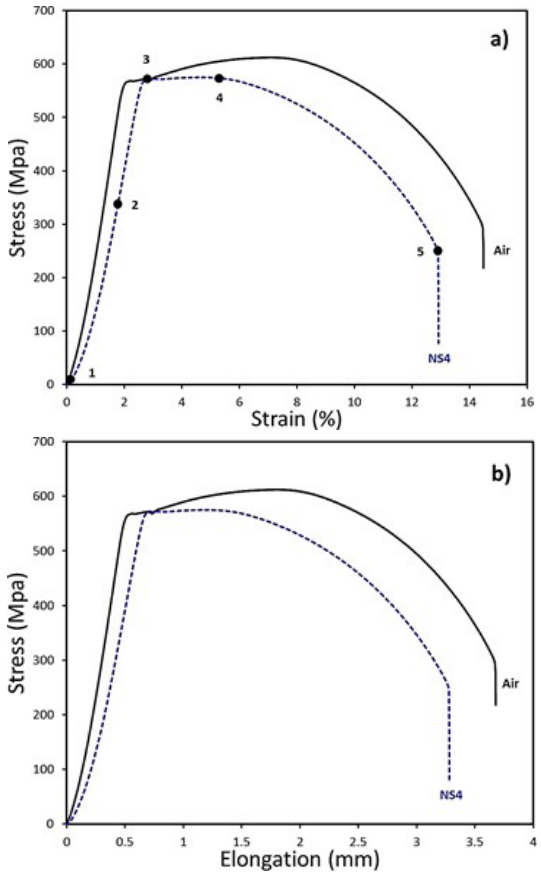

Figure 2. *a) Stress-strain profiles for X70 steel in air and exposed to NS4 solution showing five points for EN measurements, 1) beginning of the test, 2) elastic zone, 3) yielding strength, 4) ultimate tensile strength, 5) before of the fracture; b) Stress-elongation profiles for X70 steel in air and exposed to NS4 solution.*

Figure 2a shows the stress-strain curves obtained from SSRT in air and NS4 solution at room temperature showing five points where EN measurements were carried out. Figure 2b shows stress-elongation curves obtained from SSRT in air and NS4 solution. The specimens tested in air showed the higher strain and elongation compared to those tested in the NS4 solution. After perform the SSRT, the mechanical properties of these curves were obtained. Table 1 shows the mechanical properties obtained for each test condition. These mechanical properties will be used to evaluate the SCC susceptibility.

Table 1. *Mechanical properties obtained from the SSRT.*

Condition	TF	YS	UTS	ε	EL	RA	PE
	(h)	(MPa)	(MPa)	(%)	(mm)	(%)	(%)
Air	42.2	566	612	14.5	3.67	84	13.2
NS4	37.6	564	575	12.9	3.28	78	11.7

TF=time to failure, **YS**=yielding strength (0.2% ε), **UTS**=ultimate tensile strength, **ε**=strain, **EL**=elongation, **RA**=reduction area, **PE**=plastic elongation.

3.3. SCC susceptibility

Steel susceptibility to SCC is obtained evaluating its mechanical properties in a specific medium with respect to these properties in a controlled environment like air. For all the SSRT changes in time to failure ratio (TFR), reduction in area ratio (RAR), plastic elongation ratio (PER) were obtained. [19,28]

The susceptibility to SCC was expressed in terms of the percentage reduction in area (%RA) calculated by the following expression according to the NACE TM-0198 standard:

$$\%RA = \frac{\left(D_i^2 - D_f^2\right)}{D_i^2} x100 \qquad (1)$$

where D_i and D_f are the initial and the final diameters of the tensile specimen, respectively.

The reduction area ratio (RAR) after fracture for the specimen in the test environment (Ra_e) to the corresponding value determined in the controlled environment (RA_c) was calculated according to the following expression:

$$RAR = \frac{RA_e}{RA_c} \qquad (2)$$

Additionally, the time to failure ratio (TFR) was evaluated in order to have other comparison parameter of the SCC susceptibility.

$$TFR = \frac{TF_e}{TF_c} \qquad (3)$$

where TF_e is the time to failure determined for the material in the test environment and TF_c is the time to failure to the corresponding value determined in the controlled environment (air).

In similar way the plastic elongation ratio (PER) was calculated according to the following equations:

$$\%PE = \left[\frac{E_F}{L_I} - \left(\frac{\sigma_F}{\sigma_{PL}}\right)\left(\frac{E_{PL}}{L_I}\right)\right] x100 \qquad (4)$$

$$PER = \frac{PE_e}{PE_c} \quad (5)$$

Where:
PE = Plastic strain to failure (%)
E_F = Elongation at failure 2.54 (mm)
E_{PL} = Elongation at proportional limit 2.54 (mm)
L_I = Initial gauge length 2.54 (mm)
σ_F = Stress at failure (MPa)
σ_{PL} = Stress at proportional limit (MPa)

Additionally to different ratios obtained, SEM observations of the gage section of SSRT specimens were performed to observe if cracks are present, especially for tests where ratios are below 0.8. The index values of TFR, RAR and PER from 0.8 to 1 indicate that the steel has good resistance to SCC and values lower than 0.8 indicate that the steel could be susceptible to SCC. [19,28] According to the SCC index presented in Table 2, the X70 steel exposed to NS4 solution have low susceptibility to SCC. However, the RAR present an SCC index (I_{scc}) lower than 0.8, which means that steel could be susceptible to SCC. In this case it is necessary to corroborate this asseveration through SEM observations.

Table 2. *SCC index obtained from mechanical properties of SSRT.*

Condition	TF (h)	RA (%)	PE (%)	TFR	RAR	PER	I_{scc}
Air	42.2	84	13.2				
NS4	37.6	58.5	11.7	0.89	0.70	0.89	0.90

3.4. Surface fracture and longitudinal cracks observation

The complexity of cracking phenomena in a steel results from the dependence of SCC susceptibility and hydrogen induced cracking (HIC) on multiple metallurgical, mechanical, and environmental parameters that may all influence both crack initiation and propagation; which include composition, microstructure, and non-metallic inclusions in the steel, applied stress, composition of the electrolyte, among others. Figure 3 shows SEM images of the fracture surfaces of X70 steel after carried out the SSRT in air and in the synthetic soil solution. The SSRT of the X70 steel in air presented a ductile fracture, and it is characterized by extensive plastic deformation and neck formation before failure as is shown in Figure 3a. This mechanism

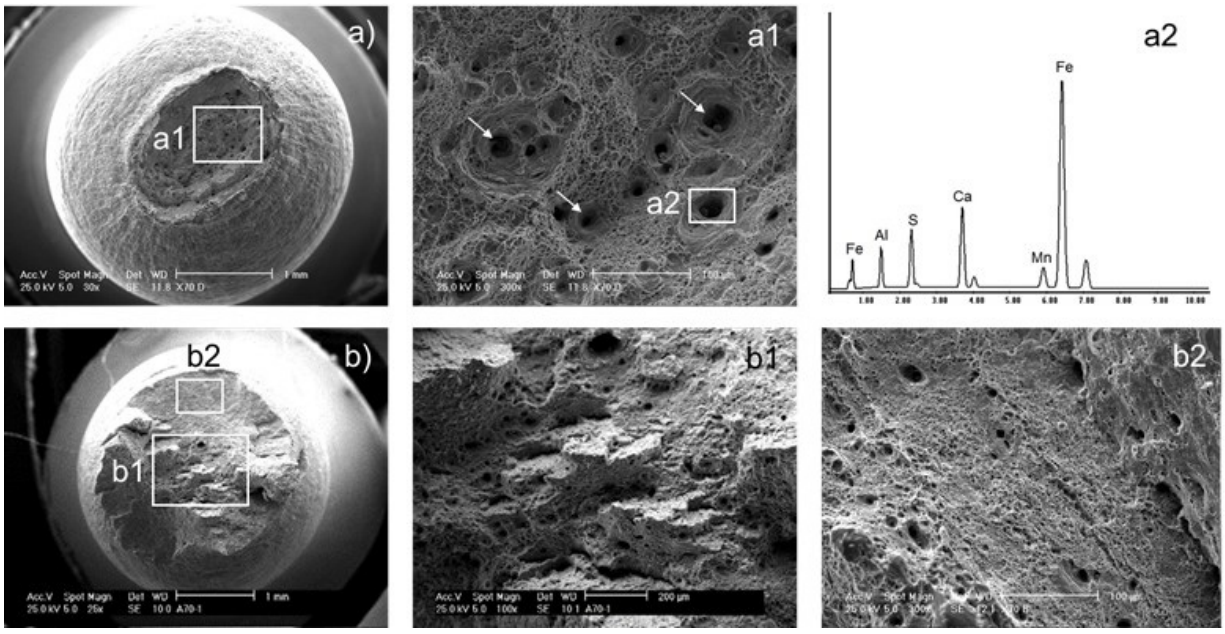

Figure 3. *SEM images showing the surface fracture from X70 steel samples tested a) in air b) NS4 solution.*

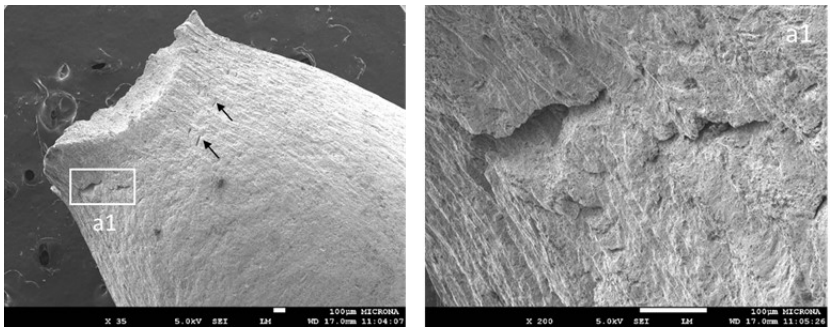

Figure 4. *SEM images of the longitudinal sections close to surface fracture showing some micro-cracks in the gage section.*

of ductile fracture is known as microvoid coalescence. [29,30] In this type of failure, microvoids in the metal act as stress concentrators being these sites where cracks initiated. These voids grow until adjacent voids connect; coalescing into larger voids until final failure of the material occurs when the voids grow larger and connect. Many cavities produced by inclusions and micro-plastic deformation can be observed in Figure 3(a1); Figure 3(a2) shows an energy dispersive spectroscopy (EDS) analysis of these inclusions. In this type of failure, microvoids (sometimes produced by inclusions) in the metal act as stress concentrators being these sites where corrosion or cracks may initiate.

The SSRT of the X70 in NS4 solution presented a mixed brittle and ductile fracture as is shown in Figure 3b. A minor neck formation in surface fracture was observed. However, a faceted fracture surface can be observed, which is indicative of a brittle type of fracture. However, the SCC susceptibility of X70 steel exposed to NS4 solution is low.

Because of low I_{scc} for RAR, some observations through SEM were carried out in the longitudinal sections of SSRT specimens. Figure 4 shows some images of the gage section of the SSR specimen close to surface fracture. SEM observations revealed the presence of some micro- cracking in the gage section, which could be attributed to micro-deformation in this area. SEM observation it is very important to be sure if cracks are presented; and it is recommended when there is ratios lower than 0.8. In the last years several studies have been carried out using SSRT and to interpret the results various criteria have been propose elsewhere. [31]

3.5. Potentiodynamic polarization curves

In order to assess the stress corrosion cracking (SCC) and to have better understanding on SCC susceptibility, polarization curves (PC) of X70 pipeline steel exposed to NS4 solution, at room temperature and atmospheric pressure were carried out. Figure 5 shows the PC obtained at different sweep rate (sweep fast: 50 mV/s and slow sweep: 0.5 mV/s) for X70 pipeline steel immersed in NS4 solution.

According to Parkins [32] during the fast sweep, the time is really short and there is not enough time to formation of a corrosion products film and subsequently absorbed it on surface of the metallic sample. This fact indicates that the surface of the steel is active and constantly corroding, simulating the crack tip. On the other hand, in slow sweep, the formation of a corrosion products film on surface of the steel is favored, and in this case, the process tried to simulate the wall of the crack. The difference between sweep rates is the driving strength for the anodic dissolution in the crack tip, and the level of SCC susceptibility of the pipeline steel.

In the slow sweep, the anodic polarization curves shows an active-passive transition state (it can be observed with a circle in the polarization curve) in the range of -690 to -610 mV vs SCE; such transition has been observed in anodic polarization curves obtained from media that promote high pH SCC. [33] According to Fu *et* al. [34] the peak indicated in Figure 5 can be attributed to the formation of Fe $(OH)_2$ deposits on the surface, which can then react with the bicarbonate ion (Eq. 6) and become an insoluble layer of $FeCO_3$ that can inhibit the anodic solution:

$$Fe(OH)_2 + HCO_3^- \rightarrow FeCO_3 + H_2O + OH^- \quad (6)$$

At sweep rate of 0.5 mV/s, the corrosion potential (E_{corr}) was -774 mV vs SCE; when the sweep rate increased to 50 mV/s the cathodic reaction was inhibited because the Ecorr and the PC were move to cathodic side and the electrochemical reactions reached a new quasi-equilibrium state (E_{corr} = -850 mV vs SCE). [35] Both anodic curves shown that the X70 pipeline steel suffered active dissolution, however according to Parkins, [32] the divergence between both curves was not enough to get a high potential to enhance SCC.

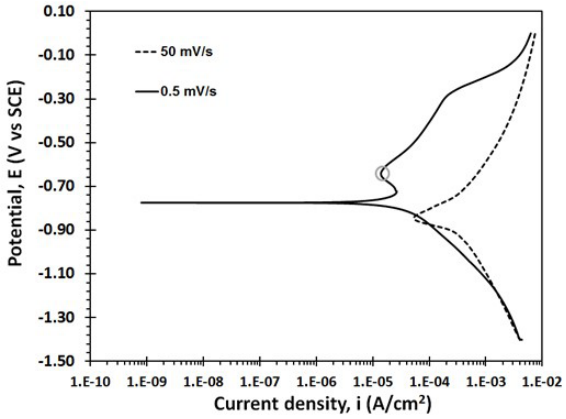

Figure 5. *Polarization curves obtained at different sweep rate for X70 pipeline steel immersed in NS4 solution.*

3.6. Electrochemical noise (EN)

Figure 2 shows five different points in the stress-strain curve where the EN measures were carried out. These points are a) at beginning of the test, b) elastic zone, c) at yield strength (YS), d) at ultimate tensile strength (UTS) and e) before rupture (RS).

Electrochemical noise were used to investigate the development of SCC process, and was evaluated at the same time of SSRT was running. The EN measured was analyzed in time and frequency domain. In time domain the analysis of E and I transients, localized index (LI) and noise resistance were the statistical methods used to study the EN. On the other hand, noise impedance was the method used in frequency domain.

3.6.1.Current (I) and potential (E) transients

Electrochemical current noise (I) and electrochemical potential noise (E) were recorded simultaneously. Figure 6 shows the current and potential transients of X70 pipeline steel of the electrochem-

ical noise measured during the SSR tests. All EN measurements were carried out in five points from stress–strain profiles shown in Figure 2. Figure 6a shows the E and I transients at the beginning of the SSR test. In this point the transients have a tendency to decrease in order to get a stable value; this behavior is attributed to the natural tendency to get stability between the anodic and cathodic reactions at the corrosion potential. It is important to point out that the current and potential transients were really small, but they were more frequent and trending to a stable value. Figure 6b, 6c and 6d showed current transients with major amplitude and more frequency than at the beginning of the test. This behavior indicates an increment of the corrosion process as the SSRT has been car-

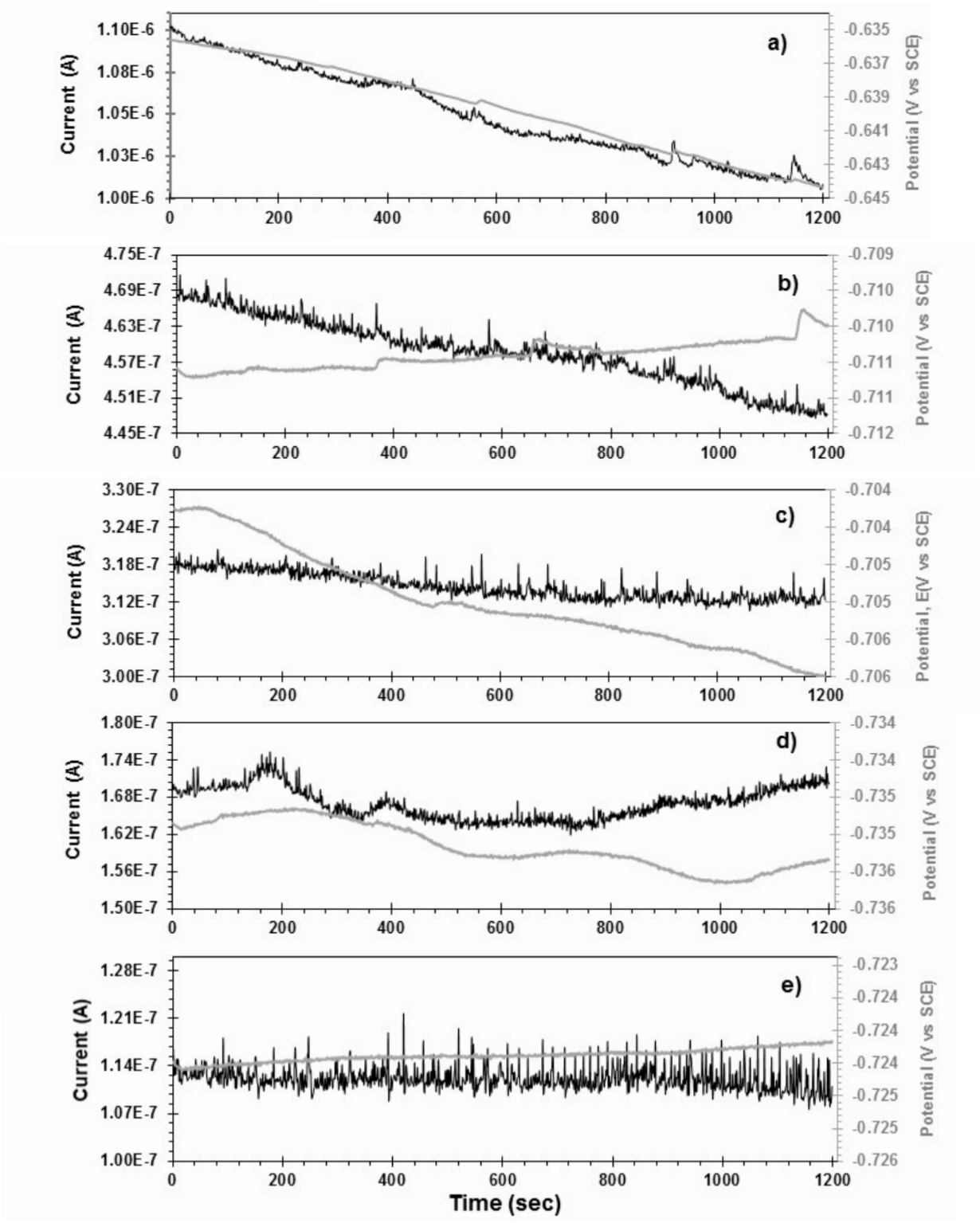

Figure 6. *Current and potential transients of EN for X70 steel in NS4 solution obtained during SSRT at: a) beginning of the test, b) elastic zone, c) YS, d) UTS and e) before of the fracture.*

rying out. Figure 6e, before of the fracture, shows currents transients with the highest amplitude and frequency. This fact indicates that the highest corrosion rate (CR) was obtained just before of the fracture.

In general, is possible to point out that during all SSRT, the potential transients had low amplitude (range from 0.03 to 0.05 mV approximately) and the currents transients also had low amplitude (8-12 μA) with no much frequency, but as the SSRT was running, the frequency of these current transients increased. This behavior could be attributed to the occurrence of events associated to localize corrosion process mainly the nucleation and initiation of microcracks. Perhaps reducing the strain rate during SSRT helps to nucleate and grow more cracks that can be detected through EN. According to Breimesser et al. [36] SCC is characterized by several transient types, distinguishable by amplitude, duration and charge, which indicate different corrosion or cracks processes. Although the steel and experimental conditions were different, transient shapes and occurrence frequencies showed a similar characteristic behavior.

Nodaways, the EN measurements to detect and monitor SCC processes on the laboratory using tensile tests has been used in several research works. [9-15,35-40]

According to Bertocci et al. [41-43] some SCC mechanisms indicate that the cracks can propagate in continuous way with a constant speed with active surface generation in the crack tip, thus the continuous propagation of this crack can provide information about electrochemical noise, specifically transients with really low amplitude and low frequency corresponding to the potential and current signals, such is the information showed in the present research and for that reason is possible to say that in spite of that EN data have low amplitude and frequency, the microcracks generated in the SSRT indicate a localized corrosion process.

3.6.2 Localized index (LI)

LI is the distribution measure data around of the root mean square of current. Equation 7 shows the parameters used in the calculation of LI.

$$LI = \sigma_I / RMS_I \quad (7)$$

Where σ_I and RMS_I is the standard deviation and root mean square of current.

LI has values from 0 to 1. Where Values close to 1 indicate localized corrosion, whereas, values close to 0 indicate general corrosion. [8,44] Table 3 shows the values range for LI and its relation with the corrosion type according with the morphology of the attack. Table 4 shows the LI values calculate by EN data obtained by X70 pipeline steel corrosion in NS4 solution. These LI are presented as a function of the conditions on the stress–strain profile. The LI values showed in this table indicate that the corrosion type from the beginning of the test until yield strength region correspond to a general corrosion type. This behavior is attributed to two factors, first of all, to the fact that a corrosion products film was adsorbed on surface of the steel sample provoking low current signals, remembering that the NS4 solution has carbonates. Second, the current signal of X70 pipeline steel in NS4 solution has really low amplitude and low frequency [41-44] as was showed in Figure 6. The LI values in the region of UTS and before the fracture indicate that a mix process dominates the total corrosion process. Thus, the steel sample in these two conditions is attacked by general and localized corrosion. The general corrosion is attributed to the corrosion products film that it was adsorbed on surface of the steel and the localized corrosion is attributed to the cracking induced by SCC. It is important to point out that the mix corrosion process begin in UTS region for that reason is possible to note that the nucleation (it should be by pitting) and formation of the crack were in the plastic zone of the stress–strain profile.

Table 3. *Correlation between localized index (LI) and corrosion type.*

LI values range	Corrosion type
0.001 < LI < 0.01	General corrosion
0.01 < LI < 0.1	Mix corrosion
0.1 < LI < 1.0	Localized corrosion

Table 4. *Localization index as a function of conditions on the stress–strain profile.*

Condition	LI
Beginning of the tests	0.004
Elastic zone	0.003
Yield strength	0.003
UTS	0.014
Before of the fracture	0.015

3.6.3. Electrochemical noise resistance (Rn)

Noise resistance was calculated at selected conditions of the stress–strain profile. R_n was estimated from the potential and current time records [8,45,46] and was calculated according to equation 8.

$$Rn = \sigma_E / \sigma_I \quad (8)$$

Where σ_E the standard deviation of potential.

Then, corrosion rate (CR) was calculated by dividing the theoretical Stern-Geary constant (B =0.120 V) by the estimated R_n values [47,48] and finally, the current obtained was divide by the total exposure area in order to get the current density. Figure 7 shows the CR obtained from electrochemical noise resistance (Rn), and the stress profile versus time. This figure shows that in the first corrosion values (beginning of the test, elastic zone and yield strength) the CR decreased. Later in the plastic region (UTS)

and before rupture, the CR increased in a considerable form, to finally, get the maximum CR before failure. In addition, where the steel sample is under stress in the elastic zone, some crystal defects, like dislocations, oscillate around its equilibrium positions, but they do not move provoking with this behavior that the interface electrolyte-metal not to be affected and the corrosion products film can formed on surface of the steel generating low signal of electrochemical noise current. In the UTS and just before the fracture, the electrochemical noise currents increase, this behavior should be attributed to the nucleation and subsequently formation of the cracks. It is important to point out that when the stress in the SSRT exceeds the elastic limit of the steel sample, a significant movement of the dislocations occur and active places are generated on surface of the steel [2] provoking the rupture of the corrosion products film adsorbed on surface of the steel and mainly it collaborate actively in the formations of the cracks.

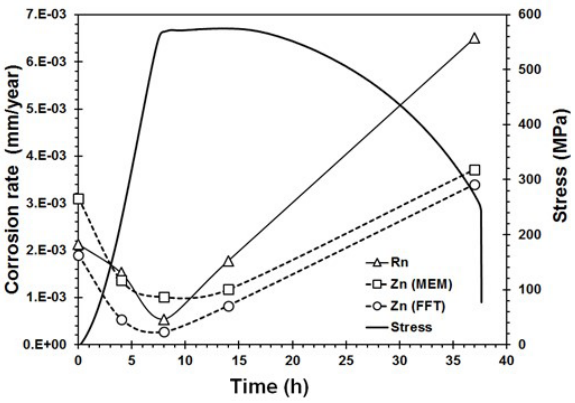

Figure 7. *Stress profile and CR as a function of the time. CR was obtained by Zn and Rn in NS4 solution. Five conditions where used: beginning of the test, elastic zone, YS, UTS and before of the fracture.*

3.6.4. Electrochemical noise impedance (Zn)

In frequency domain, the electrochemical noise analysis was carried out transforming the domain time data to power spectrum. Spectral estimation is the process of estimating the amplitude of the various frequencies present in a signal (power spectrum). There are many ways in which a power spectrum can be estimate, but two are commonly used with electrochemical noise signals, the Fourier transform in the form of Fast Fourier Transform (FFT) and maximum entropy method (MEM). As the methods are commonly used, FFT produces noisy spectra, whereas the MEM produces smoother spectra. [8] According to equation 9 is possible to estimate the Z_n values [44]

$$Zn = \sqrt{\frac{PSD_E}{PSD_I}} \qquad (9)$$

Where PSD_E and PSD_I are the power spectrum density of the potential and current respectively. Figure 7 also shows the CR obtained from electrochemical noise impedance (Zn), and the stress profile versus time. The behavior of CR values obtained by Zn is similar to the behavior of the CR values obtained by Rn. The CR at the beginning of the test, in the elastic zone and in the yield strength tends to decrease. From YS and UTS zone, the CR start to increase, to finally get the maximum CR before fracture. These behaviors indicate that conditions on SSRT to form cracks are obtained. From UTS and just before the fracture, the electrochemical noise currents increases, these should be attributed to the nucleation and subsequently formation of cracks. It is important to note that when the stress, in the SSRT exceeds the elastic limit of the steel sample the movement of the dislocations can produce cracks that they accelerate the corrosion process.

In general is possible to say that the behavior of CR of the steel sample obtained in the time domain (Rn) and frequency domain (Zn) are similar and they are agree with the analysis of the potential and current transients and LI results. Thus, the current transients and LI results indicating that low electrochemical noise current signals were obtained at the first three conditions of the SSRT and from YS and UTS until fracture, the electrochemical noise current signals were higher and these were attributed to the nucleation and formation of micro-cracks.

4. CONCLUSIONS

Electrochemical current and potential noise measurements were performed on API X70 pipeline steel samples during SSRT in order to monitor the SCC process. According to electrochemical noise study, is possible to say that the fluctuations of electrochemical noise current during the first three stages of the strain-stress curves (beginning of the test, elastic zone, YS), the corrosion process is dominate by general corrosion, but this fact is not entirely true, because this behavior really has a great influence of the localized corrosion, and the performance of the current in the corrosion process is mainly attributed to the fact that a corrosion products film that covered the surface of the steel sample and the microcracks can generate electrochemical noise current with low frequency and also low amplitude. From YS and UTS until before the fracture, the electrochemical noise current increase and consequently the corrosion rate also increased. Localization index increased during the straining (in YS and UTS mainly), indicating the presence of localized events such as pits or cracks. This behavior is attributed to the nucleation and formation of some microcracks. A superficial analysis by SEM revealed the presence of some micro-cracking in the gage section of SSRT specimens. According to SCC index, SEM observations and electrochemical study, the X70 steel has low SCC susceptibility at the conditions studied.

ACKNOWLEDGMENTS

The authors would like to thank the National Council of Science and Technology (CONACYT) for the grant awarded to Andres Carmona, required to develop this work.

REFERENCES

1. Wang, L. W.; Du, C. W.; Liu, Z. Y.; Wang, X. H.; Li, X. G.; Influence of Carbon on Stress Corrosion Cracking of High Strength Pipeline Steel , Corros. Sci., 2013, *76*, 486-493.
2. Cheng, Y. F.; Stress corrosion cracking of pipelines, John Wiley & Sons, Canada, 2013.
3. Asher, S. L.; Investigating the Mechanism of Transgranular Stress Corrosion Cracking in Near-Neutral pH Environments on Buried Fuel Transmission Pipelines, Ph.D. Dissertation, Georgia Institute of Technology, Atlanta, U.S.A., 2007.
4. Zhang, T.; Zhao, W.; Deng, Q.; Jiang, W.; Wang, Y.; Wang, Y.; Jiang, W.; Effect of Microstructure Inhomogeneity on Hydrogen Embrittlement Susceptibility of X80 Welding HAZ under Pressurized Gaseous Hydrogen, Int. J. Hydrogen Ener., 2017, 42, 25102-25113.
5. Zhang, T.; Zhao, W.; Li, T.; Zhao, Y.; Deng, Q.; Wang, Y.; Jiang, W.; Comparison of Hydrogen Embrittlement Susceptibility of Three Cathodic Protected Subsea Pipeline Steels from a Point of View of Hydrogen Permeation, Corros. Sci., 2018, *131*, 104-115.
6. Zhao, W.; Zhang, T.; Zhao, Y.; Sun, V.; Wang, Y.; Hydrogen Permeation and Embrittlement Susceptibility of X80Welded Joint under High-pressure Coal Gas Environment, Corros. Sci., 2016, *111*, 84-97.
7. Ma, H.C.; Liu, Z.Y.; Du, C.W.; Wang, H.R.; Li, X.G.; Zhang, D.W.; Cui, Z.Y.; Stress Corrosion Cracking of E690 Steel as a Welded Joint in a Simulated Marine Atmosphere containing Sulphur Dioxide, Corros. Sci., 2015, *100*, 627-641.
8. Loto, C. A., Electrochemical Noise Measurement and Statistical Parameters Evaluation of Stressed a-Brass in Mattsson's Solution, Alexandria Eng. J., 2018, *57*, 483-490.
9. Cottis, R. A. and C. A. Loto, Electrochemical Noise Generation during SCC, Mater. Sci. Forum, 1986, *8*, 201-213.
10. Gonzalez-Rodriguez, J. G.; Casales, V.; Salinas-Bravo, V. M.; Espinosa-Medina, M. A.; Martinez-Villafañe, A.; Electrochemical Noise Generated during the Stress Corrosion Cracking of Sensitized Alloy 690, J. Solid State. Chem., 2004, 8, 290-295.
11. Breimesser, M. S.; Microelectrochemical Approach Towards the Analysis of Electrochemical Noise Signals related to Intergranular Stress Corrosion Cracking of Austenitic Stainless Steel, Ph.D.; Dissertation, Universität Erlangen-Nurnberg, Germany, 2012.
12. Gonzalez-Rodriguez, J. G.; Salinas-Bravo, V. M.; Garcia-Ochoa, E.; Diaz-Sanchez, A.; Use of Electrochemical Potential Noise to Detect Initiation and Propagation of Stress Corrosion Cracks in a 17-4 PH Steel, Corrosion, 1997, 53, 693- 699.
13. Kim, J. J.; Cho, S. J.; Detection of Stress Corrosion Cracking of a Martensitic Stainless Steel by Electrochemical Noise Analysis, J. Mater. Sci. Lett., 2003, 22, 865-867.
14. Du, G.; Li, J.; Wang, W. K.; Jiang, C.; Song, S. Z.; Detection and Characterization of Stress-Corrosion Cracking on 304 Stainless Steel by Electrochemical Noise and Acoustic Emission Techniques, Corros. Sci., 2011, 53, 2918-2926.
15. Zhao, R.; Zhang, Z.; Shi, J.B.; Tao, L.; Song, S.Z.; Characterization of Stress Corrosion Crack Growth of 304 Stainless Steel by Electrochemical Noise and Scanning Kelvin Probe, J. Central South U. Technol., 2010, 17, 13-18.
16. Kovacˇ, J.; Legat, A.; Zajec, B.; Kosec, T.; Govekar, V.; Detection and Characterization of Stainless Steel SCC by the Analysis of Crack related Acoustic Emission, Ultrasonics, 2015, 62, 312-322.
17. Cottis, R. A.; The Significance of Electrochemical Noise Measurements on Asymmetric Electrodes, Electrochim. Acta, 2007, 52, 7585- 7589.
18. Contreras, A.; Salazar, M.; Carmona, A.; Galván-Martínez, Electrochemical Noise for Detection of Stress Corrosion Cracking of Low Carbon Steel Exposed to Synthetic Soil Solution, R.; Mater. Res.-Ibero-am. J. Mater., 2017, 1201-1210.
19. NACE TM-0198 (2016), Slow strain rate test method for screening corrosion-resistant alloys for stress corrosion cracking in sour oilfield service, NACE International, Houston, TX, U.S.A. 2016.
20. Li, X.C.; Eadie, R.L.; Luo, J.L.; Influence of Plasticity on Corrosion and Stress Corrosion Cracking Behaviour in Near Neutral pH Environment, Corros. Eng.Sci. Technol., 2008, 43, 297-303.
21. Bueno, A.H.S.; Moreira, E.D.; Siqueira, P.; Gomes, J.A.C.P.; Effect of Cathodic Potential on Hydrogen Permeation of API Grade Steels in Modified NS4 Solution, Mater. Sc. Eng. A, 2014, 597, 117-121.
22. Wan, H.; Song, D.; Liu, Z.; Du, C.; Zeng, Z.; Yang, X.; Li, X.; Effect of Alternating Current on Stress Corrosion Cracking Behavior and Mechanism of X80 Pipeline Steel in Near-Neutral Solution, J Nat. Gas Sc. Eng., 2017, 38, 458-465.
23. ASTM G1-03 (2017) Standard practice for preparing, cleaning, and evaluating corrosion test specimens, ASTM International, West Conshohocken, PA, U.S.A. 2017.
24. Omura, T.; Amaya, H.; Asahi, H.; Sawamura, V.; Kimura, M. Proceeding of CORROSION 09, Paper No. 09092, Georgia, U.S:A., March 22-26, pp. 1-16, 2009.
25. Sawamura, M.; Asahi, H.; Omura, T.; Kishikawa, H.; Ishikawa, N.; Kimura, M. Proceeding of CO-

RROSION 2011, Paper No. 11286, Houston, TX, U.S.A., March 13-17, pp. 1-13, 2011.
26. Asahi, H.; Kushida, T.; Kimura, M.; Fukai, H.; Okano, S.; Role of Microstructures on Stress Corrosion Cracking of Pipeline Steels in Carbonate-Bicarbonate Solution, Corrosion, 1999, 55, 644-652.
27. Gonzalez-Rodriguez, J.G.; Casales, M.; Salinas-Bravo, V.M.; Albarran, J.L.; Martinez, L.; Effect of Microstructure on the Stress Corrosion Cracking of X-80 Pipeline Steel in Diluted Sodium Bicarbonate Solutions, Corrosion, 2002, 58, 584-590.
28. ASTM G-129 (2013) Slow strain rate testing to evaluate the susceptibility of metallic materials to environmentally assisted cracking, ASTM International, West Conshohocken, PA, U.S.A. 2016.
29. Contreras, A.; Sosa, E.; Espinosa, M.A.; Cathodic Protection Effect on the Assessment of SCC Susceptibility of X52 Pipeline Steel, Mat. Res. Soc. Proceedings, 2010, 1242, 43-53.
30. Contreras, A.; Hernández, S. L.; Orozco-Cruz, R.; Galvan-Martínez, R.; Mechanical and Environmental Effects on Stress Corrosion Cracking of Low Carbon Pipeline Steel in a Soil Solution, Mater Design, 2012, 35, 281-289.
31. Kane, R. D.; Joia, C.J.B.M.; Small, A.L.T.; Ponciano, J.; Rapid Screening of Stainless-Steels for Environmental Cracking, Mater Performance. 1997, 36, 71-74.
32. Parkins, R. N.; Predictive Approaches to Stress Corrosion Cracking Failure, Corros. Sci., 1980, 20, 147-166.
33. Beavers, J. A.; Jaske, C.E.; Proceeding of CORROSION 99, Paper No. 142, TX, U.S.A., April 25-30, pp. 1-24, 1999.
34. Fu, A. Q.; Cheng, Y.F.; Electrochemical Polarization Behavior of X70 Steel in Thin Carbonate/Bicarbonate Solution Layers Trapped under a Disbonded Coating and its Implication on pipeline SCCCorros. Sci., 2010, 52, 2511-2518.
35. Liu, Z. Y.; Li, X. G.; Cheng, Y. F.; Mechanistic Aspect of Near-Neutral pH Stress Corrosion Cracking of Pipelines under Cathodic Polarization, Corros. Sci., 2012, 55, 54-60.
36. Breimesser, M.; Ritter, S.; Seifert, H.P.; Suter, T.; Virtanen, S.; Application of Electrochemical Noise to Monitor Stress Corrosion Cracking of Stainless Steel in Tetrathionate Solution under Constant Load, Corros. Sci., 2012, 63, 129-139.
37. Kovac, J.; Alaux, C.; Marrow, T.J.; Govekar, E.; Legat, A.; Correlations of Electrochemical Noise, Acoustic Emission and Complementary Monitoring Techniques During Intergranular Stress-Corrosion Cracking of Austenitic Stainless Steel, Corros. Sci., 2010, 52, 2015-2025.
38. Leban, M.; Bajt, Å.; Legat, A.; Detection and Differentiation Between Cracking Processes. Based on Electrochemical and Mechanical Mea -surements; Electrochim. Acta, 2004, 49, 2795-2801.
39. Ritter, S.; Seifert, H.P.; Detection of SCC Initiation in Austenitic Stainless Steel by Electrochemical Noise Measurements, Mat. Corros., 2013, 64, 683-690.
40. Ortiz Alonso, C.J.; Lucio–Garcia, M.A.; Hermoso-Diaz, I.A.; Chacon-Nava, J.G.; Martinez- Villafañe, A.; Gonzalez-Rodriguez, J.G.; Detection of Sulfide Stress Cracking in a Supermartensitic Stainless Steel by using Electrochemical Noise; Int. J. Electrochem. Sci., 2014, 9, 6717-6733.
41. Bertocci, U.; Huet, F.; Noise Analysis Applied to Electrochemical Systems; Corrosion, 1995, 51, 131-144.
42. Bertocci, U.; Gabrielli, C.; Huet, F.; Keddam, M.; Noise Resistance Applied to Corrosion Measurements; J. Electrochem. Soc. 1997, 144, 31-37.
43. Bertocci U.; Hue, F.; Noise Resistance Applied to Corrosion Measurements: IV. Asymmetric Coated Electrodes; J. Electrochem. Soc. 1997, 144, 2786-2793.
44. Cottis, R. A.; Interpretation of Electrochemical Noise Data; Corrosion, 2001, 57, 265-285.
45. Galvan-Martinez, R.; Orozco-Cruz, R.; Mendoza-Flores, J.; Genesca-Llongueras, J.; Contreras-Cuevas, A.; Electrochemical Noise Study on Corrosion of Low Carbon Pipeline Steel in Sour Solutions; Mater. Sci. Forum, 2014, 793, 67-76.
46. Xia, D.H.; Ma, C.; Song, S.; Ma, L.; Wang, J.; Gao, Z.; Zhong, C.; Hua, W.; Assessing Atmospheric Corrosion of Metals by a Novel Electrochemical Sensor combining with a Thin Insulating Net using Electrochemical Noise Technique; Sensors and Actuators B: Chemical, 2017, 252, 353-358.
47. Jamalia, S. S.; Millsa, D. J.; Sykes, J. M.; Measuring Electrochemical Noise of a Single Working Electrode for Assessing Corrosion Resistance of Polymer Coated Metals; Prog. Org. Coat., 2014, 77, 733-741.
48. Cuevas-Arteaga, C.; Porcayo-Calderon, j.; Electrochemical Noise Analysis in the Frequency Domain and Determination of Corrosion Rates for SS-304 Stainless Steel; J.; Mat. Sci. Eng. A, 2006, 435–436, 439-446.